Supporting Information
Small-to-Large Length Scale Transition of TMAO Interaction with Hydrophobic Solutes

Angelina Folberth*, Swaminath Bharadwaj, and Nico F. A. van der Vegt*

Contents

Eduard-Zintl-Institut fuer Anorganische und Physikalische Chemie, Technical University of Darmstadt, Alarich-Weiss-Strasse 10, 64287 Darmstadt, Germany
E-mail: folberth@cpc.tu-darmstadt.de; vandervegt@cpc.tu-darmstadt.de

S1 Association of polyalanine helices

The potential of mean force (PMF) between two polyalanine-helices is shown in Fig. S1. The configuration of the associated helices at around 0.85 nm was randomly taken from the first minimum of the PMF, where the helices are in contact and mainly interact via van der Waals interactions. The second minimum at around 1.05 nm corresponds to a solvent-shared helix pair, where one layer of water molecules separates the solutes.

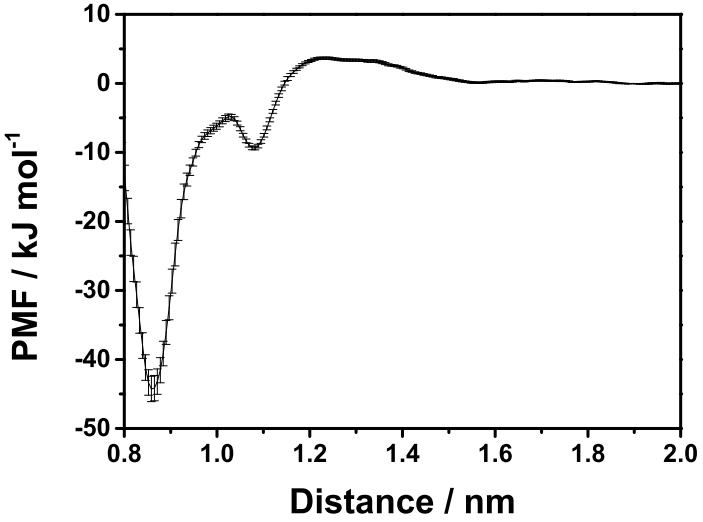

Fig. S1 PMF between the center of mass of two polyalanine-helices in water obtained via umbrella sampling.

S2 Free energy calculations

The solvation free energy ΔG of the polyalanine-helices in water-TMAO mixtures was computed using free energy perturbation (FEP) and thermodynamic integration (TI). The solvation process can be considered as a two step thermodynamic process where a repulsive cavity is created to host the solute and subsequently solute-solvent cohesive interactions are introduced. The contribution to the solvation free energy from the solute-solvent cohesive interactions can be further subdivided into contributions from cohesive solute-solvent van der Waals interactions and solute-solvent electrostatic interactions. The solvation free energy is then

$$\begin{aligned} \Delta G &= \Delta G_{\mathrm{vdW,R}} + \Delta G_{\mathrm{vdW,A}} + \Delta G_{\mathrm{Elec}} \\ \Delta G_{\mathrm{vdW}} &= \Delta G_{\mathrm{vdW,R}} + \Delta G_{\mathrm{vdW,A}} \end{aligned} \tag{S1}$$

where $\Delta G_{\mathrm{vdW,R}}$ is the reversible work of creating a repulsive cavity which has the same shape and size as the solute, $\Delta G_{\mathrm{vdW,A}}$ is the reversible work associated with subsequently introducing cohesive solute-solvent van der Waals interactions with the preformed cavity, and ΔG_{Elec} is the reversible work associated with the final introduction of solute-solvent electrostatic interactions. Note that these contributions to the solvation free energy are dependent on the sequence in which the different solute-solvent interactions are introduced. ΔG_{vdW} is the reversible work associated with introducing solute-solvent van der Waals interactions. In this work, the solute-solvent van der Waals interactions are modelled through the Lennard-Jones (LJ) potential and the solute-solvent repulsive interactions are modelled through the Weeks-Chandler-Andersen (WCA) potential.[1] The cohesive solute-solvent van der Waals interaction energy ψ_A is then given by the following expression,

$$\psi_A = \begin{cases} -\varepsilon, & r < 2^{1/6}\sigma \\ 4\varepsilon\left[\left(\frac{\sigma}{r}\right)^{12} - \left(\frac{\sigma}{r}\right)^{6}\right], & r \geq 2^{1/6}\sigma \end{cases} . \tag{S2}$$

In this work, the different contributions to ΔG were computed from a combination of two sets of simulations. From the first set of simulations, $\Delta G_{\mathrm{vdW,R}}$ was calculated. $\Delta G_{\mathrm{vdW,R}}$ can be computed by gradually introducing the solute-solvent WCA interactions. Equivalently, one can also compute $\Delta G_{\mathrm{vdW,R}}$ by gradually decoupling the solute-solvent WCA interactions through a set of $\lambda_{\mathrm{vdW,R}}$ values. The latter approach was employed in this work to compute $\Delta G_{\mathrm{vdW,R}}$. Here, $\lambda_{\mathrm{vdW,R}} = 0$ is the state where the solute-solvent WCA interactions are coupled and $\lambda_{\mathrm{vdW,R}} = 1$ is the state where solute-solvent WCA interactions are decoupled.

The second set of simulations involves two steps where first the solute-solvent LJ interactions were gradually introduced to compute ΔG_{vdW}. Subsequently, the solute-solvent electrostatic interactions were gradually introduced to compute ΔG_{Elec}. Equivalently, one can also compute these free energies by gradually decoupling the different solute-solvent interactions. Note that the solute-solvent electrostatic interactions are decoupled first and then the solute-solvent LJ interactions are decoupled. In this work, the solute-solvent

electrostatic interactions were gradually decoupled to obtain ΔG_{Elec} through a set of λ_{Elec} values where $\lambda_{\text{Elec}} = 0$ refers to the state where both solute-solvent LJ and electrostatic interactions are coupled and $\lambda_{\text{Elec}} = 1$ is the state where only solute-solvent LJ interactions are coupled. Subsequently, ΔG_{vdW} was computed by gradually decoupling the solute-solvent LJ interactions through a set of λ_{vdW} values where $\lambda_{\text{vdW}} = 0$ refers to the state where the solute-solvent LJ interactions are coupled and $\lambda_{\text{vdW}} = 1$ is the state where solute-solvent LJ interactions are decoupled. ΔG and $\Delta G_{\text{vdW,A}}$ were then computed from the following expressions,

$$\begin{aligned} \Delta G &= \Delta G_{\text{vdW}} + \Delta G_{\text{Elec}} \\ \Delta G_{\text{vdW,A}} &= \Delta G_{\text{vdW}} - \Delta G_{\text{vdW,R}} \end{aligned} \tag{S3}$$

The open source python tool "Alchemical Analysis" (AA) was employed to compute the solvation free energy and the different contributions to it.[2] The AA tool computes the solvation free energy through TI, and FEP methods such as Bennett Acceptance Ratio (BAR), Deletion Exponential Averaging (DEXP) and Insertion Exponential Averaging (IEXP).[3] The set of $\lambda_{\text{vdW,R}}$, λ_{vdW} and λ_{Elec} values were chosen in a manner which ensures that the solvation free energies calculated from these four methods were in quantitative agreement (see Sec. S3). This also ensures that the errors in the computed solvation free energies are very small (see Fig. S2(a)). Note that such an approach leads to unevenly spaced $\lambda_{\text{vdW,R}}$, λ_{vdW} and λ_{Elec} values in this work. The values of the $\lambda_{\text{vdW,R}}$, λ_{vdW} and λ_{Elec} for polyalanine-helix cavities at different TMAO concentrations are listed in the subsequent sections.

S2.1 Calculation of $\Delta G_{\text{vdW,R}}$ for the polyalanine-helix cavity

S2.1.1 Single helix

All concentrations (51 parameters)

$\lambda_{\text{vdW,R}}$ = 0.000 0.050 0.100 0.150 0.250 0.300 0.350 0.400 0.450 0.500 0.550 0.580 0.600 0.630 0.650 0.680 0.700 0.715 0.730 0.750 0.760 0.770 0.780 0.790 0.800 0.810 0.820 0.825 0.830 0.834 0.837 0.840 0.844 0.847 0.850 0.855 0.860 0.865 0.870 0.880 0.884 0.887 0.890 0.900 0.910 0.920 0.930 0.950 0.980 1.000

S2.1.2 Associated helices

All concentrations (64 parameters)

$\lambda_{\text{vdW,R}}$ = 0.000 0.050 0.100 0.150 0.200 0.250 0.300 0.350 0.400 0.450 0.500 0.550 0.575 0.600 0.625 0.650 0.675 0.700 0.710 0.720 0.730 0.740 0.750 0.760 0.770 0.780 0.790 0.800 0.810 0.820 0.830 0.840 0.845 0.850 0.855 0.860 0.865 0.870 0.872 0.874 0.876 0.878 0.880 0.885 0.890 0.895 0.900 0.905 0.910 0.915 0.920 0.930 0.940 0.945 0.950 0.955 0.960 0.965 0.970 0.975 0.980 0.985 0.990 1.000

S2.2 Calculation of ΔG_{vdW} for the polyalanine-helix

S2.2.1 Single helix

0 M (56 parameters)

λ_{vdW} = 0.000 0.050 0.100 0.150 0.200 0.250 0.300 0.350 0.400 0.450 0.475 0.500 0.525 0.550 0.575 0.600 0.625 0.650 0.670 0.690 0.700 0.710 0.720 0.730 0.740 0.750 0.760 0.765 0.770 0.775 0.778 0.780 0.782 0.784 0.786 0.788 0.790 0.795 0.800 0.805 0.810 0.820 0.830 0.840 0.850 0.860 0.870 0.880 0.890 0.900 0.910 0.925 0.940 0.950 0.970 1.000

1 M (57 parameters)

λ_{vdW} = 0.000 0.050 0.100 0.150 0.200 0.250 0.300 0.350 0.400 0.450 0.475 0.500 0.525 0.550 0.575 0.600 0.625 0.650 0.670 0.690 0.700 0.710 0.720 0.730 0.740 0.750 0.760 0.765 0.770 0.773 0.775 0.778 0.780 0.783 0.787 0.790 0.793 0.797 0.800 0.803 0.807 0.810 0.815 0.820 0.830 0.840 0.850 0.860 0.870 0.880 0.890 0.900 0.910 0.925 0.940 0.950 0.970 1.000

2 M (57 parameters)

λ_{vdW} = 0.000 0.050 0.100 0.150 0.200 0.250 0.300 0.350 0.400 0.450 0.475 0.500 0.525 0.550 0.575 0.600 0.625 0.650 0.670 0.690 0.700 0.710 0.720 0.730 0.740 0.750 0.760 0.765 0.770 0.775 0.780 0.782 0.784 0.786 0.788 0.790 0.800 0.810 0.813 0.817 0.820 0.825 0.830 0.840 0.850 0.860 0.870 0.880 0.890 0.900 0.910 0.925 0.940 0.950 0.960 0.970 0.980 1.000

3 M (54 parameters)

λ_{vdW} = 0.000 0.050 0.100 0.150 0.200 0.250 0.300 0.350 0.400 0.450 0.475 0.500 0.525 0.550 0.575 0.600 0.625 0.650 0.670 0.690 0.700 0.710 0.720 0.730 0.740 0.750 0.760 0.765 0.770 0.775 0.780 0.790 0.800 0.805 0.810 0.813 0.817 0.820 0.825 0.830 0.840 0.850 0.860 0.870 0.880 0.890 0.900 0.910 0.925 0.940 0.950 0.960 0.970 0.980 1.000

S2.2.2 Associated helices

0 M (61 parameters)

λ_{vdW} = 0.000 0.050 0.075 0.100 0.125 0.150 0.175 0.200 0.225 0.250 0.275 0.300 0.325 0.350 0.375 0.400 0.425 0.450 0.475 0.500 0.525 0.550 0.575 0.600 0.625 0.650 0.675 0.700 0.720 0.740 0.750 0.760 0.765 0.770 0.772 0.774 0.776 0.778 0.780 0.782 0.784 0.786 0.788 0.790 0.795 0.800 0.805 0.810 0.815 0.820 0.830 0.840 0.850 0.870 0.890 0.900 0.920 0.940 0.950 0.960 0.980 1.000

1 M (55 parameters)

λ_{vdW} = 0.000 0.050 0.075 0.100 0.125 0.150 0.175 0.200 0.225 0.250 0.275 0.300 0.325 0.350 0.375 0.400 0.425 0.450 0.475 0.500 0.525 0.550 0.575 0.600 0.625 0.650 0.675 0.700 0.720 0.740 0.750 0.760 0.770 0.775 0.780 0.790 0.800 0.810 0.815 0.820 0.825 0.830 0.835 0.840 0.850 0.860 0.870 0.880 0.890 0.900 0.920 0.940 0.950 0.960 0.980 1.000

2 M (60 parameters)

λ_{vdW} = 0.000 0.050 0.075 0.100 0.125 0.150 0.175 0.200 0.225 0.250 0.275 0.300 0.325 0.350 0.375 0.400 0.425 0.450 0.475 0.500 0.525 0.550 0.575 0.600 0.625 0.650 0.675 0.700 0.720 0.740 0.750 0.760 0.770 0.775 0.780 0.790 0.795 0.800 0.810 0.815 0.820 0.825 0.830 0.835 0.840 0.850 0.860 0.870 0.880 0.890 0.900 0.910 0.920 0.930 0.940 0.950 0.960 0.970 0.980 0.990 1.000

3 M (71 parameters)

λ_{vdW} = 0.000 0.050 0.075 0.100 0.125 0.150 0.175 0.200 0.225 0.250 0.275 0.300 0.325 0.350 0.375 0.400 0.425 0.450 0.475 0.500 0.525 0.550 0.575 0.600 0.625 0.650 0.675 0.690 0.700 0.710 0.720 0.730 0.740 0.750 0.760 0.770 0.775 0.780 0.790 0.795 0.800 0.805 0.810 0.813 0.817 0.820 0.823 0.827 0.830 0.835 0.840 0.845 0.850 0.855 0.860 0.865 0.870 0.875 0.880 0.885 0.890 0.900 0.910 0.920 0.930 0.940 0.950 0.960 0.970 0.980 0.990 1.000

S2.3 Calculation of $\Delta G_{\mathbf{Elec}}$ for the polyalanine-helix

S2.3.1 Single helix

0 M (20 parameters)

λ_{Elec} = 0.000 0.050 0.100 0.150 0.200 0.250 0.300 0.350 0.400 0.450 0.475 0.500 0.550 0.600 0.650 0.700 0.750 0.800 0.850 0.900 1.000

1 M (30 parameters)

λ_{Elec} = 0.000 0.025 0.050 0.075 0.100 0.125 0.150 0.175 0.200 0.225 0.250 0.275 0.300 0.325 0.350 0.375 0.400 0.425 0.450 0.475 0.500 0.550 0.600 0.650 0.700 0.750 0.800 0.850 0.900 1.000

2 M (39 parameters)

λ_{Elec} = 0.000 0.010 0.025 0.040 0.050 0.060 0.075 0.090 0.100 0.110 0.125 0.140 0.150 0.160 0.175 0.190 0.200 0.210 0.225 0.250 0.275 0.300 0.325 0.350 0.375 0.400 0.425 0.450 0.475 0.500 0.550 0.600 0.650 0.700 0.750 0.800 0.850 0.900 1.000

3 M (23 parameters)

λ_{Elec} = 0.000 0.050 0.100 0.150 0.200 0.220 0.240 0.250 0.300 0.350 0.400 0.450 0.475 0.500 0.550 0.600 0.650 0.700 0.750 0.800 0.850 0.900 1.000

S2.3.2 Associated helices

0 M (33 parameters)

λ_{Elec} = 0.000 0.025 0.050 0.070 0.100 0.120 0.150 0.170 0.200 0.220 0.250 0.270 0.300 0.350 0.400 0.450 0.500 0.520 0.550 0.570 0.600 0.620 0.650 0.670 0.700 0.720 0.750 0.770 0.800 0.850 0.900 0.950 1.000

1 M (41 parameters)

λ_{Elec} = 0.000 0.010 0.020 0.030 0.040 0.050 0.070 0.085 0.100 0.120 0.150 0.170 0.200 0.220 0.250 0.270 0.300 0.325 0.350 0.375 0.400 0.425 0.450 0.475 0.500 0.520 0.550 0.570 0.600 0.620 0.650 0.670 0.700 0.720 0.750 0.770 0.800 0.850 0.900 0.950 1.000

2 M (40 parameters)

λ_{Elec} = 0.000 0.010 0.020 0.030 0.040 0.050 0.070 0.100 0.120 0.150 0.170 0.200 0.220 0.250 0.270 0.300 0.325 0.350 0.375 0.400 0.425 0.450 0.475 0.500 0.520 0.550 0.570 0.600 0.620 0.650 0.670 0.700 0.720 0.750 0.770 0.800 0.850 0.900 0.950 1.000

3 M (32 parameters)

λ_{Elec} = 0.000 0.050 0.070 0.100 0.120 0.150 0.170 0.200 0.220 0.250 0.270 0.300 0.350 0.400 0.450 0.500 0.520 0.550 0.570 0.600 0.620 0.650 0.670 0.700 0.720 0.750 0.770 0.800 0.850 0.900 0.950 1.000

S3 Comparison of TI and BAR

We compare the results obtained from thermodynamic integration (TI)[4] and the BAR algorithm.[3,5] We have calculated $\Delta\Delta G^{\mathrm{A}}_{\mathrm{vdW}}$ and $\Delta\Delta G^{\mathrm{D}}_{\mathrm{vdW}}$ and then obtained the association solvation free energy through $\Delta\Delta G^{\mathrm{D}\to\mathrm{A}}_{\mathrm{vdW}} = \Delta\Delta G^{\mathrm{A}}_{\mathrm{vdW}} - \Delta\Delta G^{\mathrm{D}}_{\mathrm{vdW}}$. $\Delta\Delta G^{\mathrm{D}\to\mathrm{A}}_{\mathrm{vdW}}$ is an order of magnitude smaller than $\Delta\Delta G_{\mathrm{vdW}}$ and therefore very susceptible to errors in $\Delta\Delta G_{\mathrm{vdW}}$. $\Delta\Delta G^{\mathrm{D}\to\mathrm{A}}_{\mathrm{vdW,R}}$ and $\Delta\Delta G^{\mathrm{D}\to\mathrm{A}}_{\mathrm{vdW,A}}$ on the other hand are on a similar order of magnitude compared to the respective solvation free energies from which they are calculated. Therefore, the influence of the algorithm on the quantitative results can be best estimated from $\Delta\Delta G^{\mathrm{D}\to\mathrm{A}}_{\mathrm{vdW}}$. It can be seen in Fig. S2(a) that the relative solvation free energies $\Delta\Delta G_{\mathrm{vdW}}$ obtained from different algorithms are in quantitative agreement. Nevertheless, as shown in Fig. S2(b) there are still some small differences in $\Delta\Delta G^{\mathrm{D}\to\mathrm{A}}_{\mathrm{vdW}}$ obtained from TI and BAR. However, the trends remain the same.

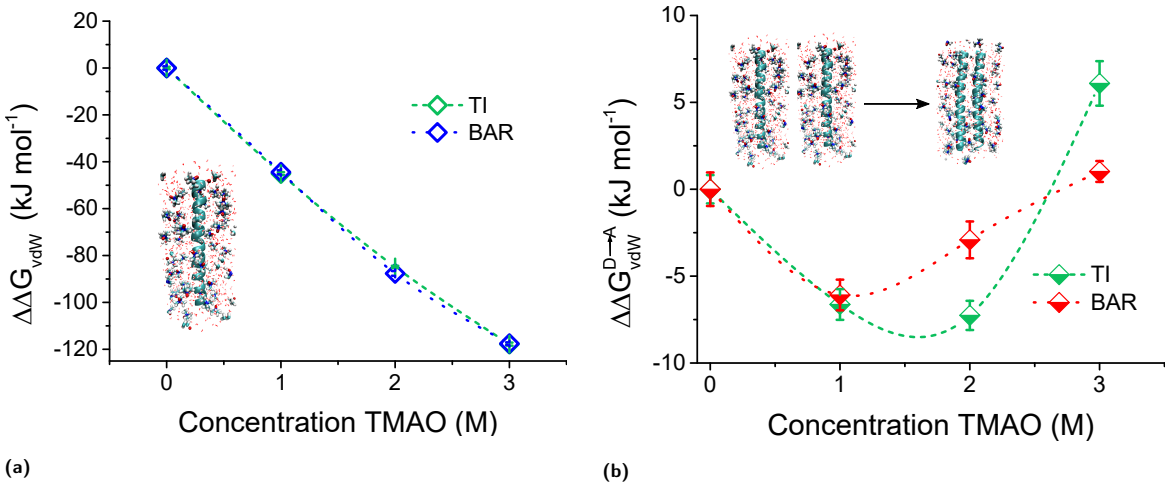

Fig. S2 a) Change in the relative solvation free energy $\Delta\Delta G_{\mathrm{vdW}}$ as a function of TMAO concentration for the single helix using TI and BAR. It can be seen that the results obtained by either analysis are in quantitative agreement. Errors are in order of the symbol size. b) Change in the relative solvation free energy $\Delta\Delta G^{\mathrm{D}\to\mathrm{A}}_{\mathrm{vdW}}$ as a function of TMAO concentration for TI and BAR. It can be seen that the trends remain the same, but there are small differences in absolute values.

S4 Solvation free energies in pure water

We have reported all solvation free energies in reference to the solvation free energy in pure water. Table S1 summarizes the different contributions to the solvation free energy in pure water.

Table S1 Solvation free energies ΔG, ΔG_{vdW}, $\Delta G_{\mathrm{vdW,R}}$, $\Delta G_{\mathrm{vdW,A}}$ and ΔG_{Elec} in pure water for the dissociated (D) and associated (A) states. Solvation free energies of the dissociated state were obtained by doubling the solvation free energy of a single helix. The solvation free energies are expressed in kJ mol^{-1}.

	Dissociated state	Associated state
ΔG	-429.2 ± 0.8	-341.0 ± 0.5
ΔG_{vdW}	105.1 ± 0.7	131.9 ± 0.2
$\Delta G_{\mathrm{vdW,R}}$	1475.0 ± 0.8	1113.2 ± 0.3
$\Delta G_{\mathrm{vdw,A}}$	-1369.9 ± 1.5	-981.3 ± 0.4
ΔG_{Elec}	-534.2 ± 0.4	-472.9 ± 0.4

S5 Solvent accessible surface area (SASA)

The SASA has been calculated using the double cubic lattice method developed by Eisenhaber et al. as implemented in GROMACS.[6] The SASA for the single helix is 24.13 nm^2 and the one of the associated helices is 37.72 nm^2. Therefore, 10.54 nm^2 of the solute surface area becomes inaccessible to the solvent upon association.

S6 Preferential binding coefficient Γ_{23}

The preferential binding coefficient Γ_{23} is defined by the following expression,

$$\Gamma_{23} = \rho_3 \left(G_{23} - G_{21}\right), \tag{S4}$$

where the index $i = 1$ stands for water, $i = 2$ for the solute and $i = 3$ for TMAO. ρ_3 is the molar concentration of TMAO, G_{23} and G_{21} are the solute-TMAO and solute-water Kirkwood-Buff integrals. TMAO is preferentially adsorbed on the solute for $\Gamma_{23} > 0$. On the other hand, the solute is preferentially hydrated for $\Gamma_{23} < 0$, i.e. TMAO is depleted from the solute. Γ_{23} can also be written in terms of the number of TMAO and water molecules in the following way,[7]

$$\Gamma_{23}(r) = \left\langle n_3(r) - \frac{N_3 - n_3(r)}{N_1 - n_1(r)} n_1(r) \right\rangle, \tag{S5}$$

where $n_3(r)$ and $n_1(r)$ are the number of TMAO and the number of water molecules within a proximal distance of r from the solute surface, respectively. N_3 and N_1 are the total number of TMAO and water molecules in the system, respectively. The preferential binding coefficients were calculated using the expression in eqn S5. The dependence of the solvation free energy, of the associated or the dissociated state, on the TMAO concentration can be related to the corresponding preferential binding coefficients through the Wyman-Tanford relations,[8,9]

$$\frac{\partial \Delta G^{\mathrm{j}}}{\partial \rho_3} = -\frac{\Gamma^{\mathrm{j}}_{23}}{\rho_3 \left(1 + \rho_3 \left(G_{33} - G_{31}\right)\right)} \tag{S6}$$

where the index j=A,D represents the associated or dissociated state, G_{33} and G_{31} are the Kirkwood-Buff integrals corresponding to the TMAO-TMAO interaction and the TMAO-water interaction, respectively. Note that the factor $1 + \rho_3 \left(G_{33} - G_{31}\right)$ is positive at all TMAO concentrations as TMAO and water form stable mixtures.[10] Preferential adsorption of TMAO ($\Gamma_{23} > 0$) leads to a decrease in the solvation free energy with increase in TMAO concentration. On the other hand, the solvation free energy increases with increase in TMAO concentration when TMAO is depleted from the solute surface, $\Gamma_{23} < 0$. Then, for the dissociation-association equilibrium, $D \rightleftharpoons A$, the dependence of the free energy change upon association, $\Delta G^{D \to A}$, on the TMAO concentration concentration can be related to the preferential binding coefficients of the associated and dissociated states in the following way

$$\left(\frac{\partial \Delta G^{\mathrm{D}\to\mathrm{A}}}{\partial \rho_3}\right)_{p,T} = -\frac{\Gamma^{\mathrm{A}}_{23} - \Gamma^{\mathrm{D}}_{23}}{\rho_3 \left(1 + \rho_3 \left(G_{33} - G_{31}\right)\right)} = -\frac{\Delta\Gamma^{\mathrm{D}\to\mathrm{A}}_{23}}{\rho_3 \left(1 + \rho_3 \left(G_{33} - G_{31}\right)\right)} \tag{S7}$$

$\Delta G^{\mathrm{D}\to\mathrm{A}}$ increases with the increase in the TMAO concentration when TMAO preferentially adsorbs on the dissociated state, i.e. $\Delta\Gamma^{\mathrm{D}\to\mathrm{A}}_{23} < 0$. This shifts the $D \rightleftharpoons A$ equilibrium towards the dissociated state. On the other hand, TMAO shifts the $D \rightleftharpoons A$ equilibrium towards the associated state when it preferentially adsorbs on the associated state ($\Delta\Gamma^{\mathrm{D}\to\mathrm{A}}_{23} > 0$), i.e. $\Delta G^{\mathrm{D}\to\mathrm{A}}$ decreases with increase in TMAO concentration.

The dissociated (single helix) and associated state have been simulated starting from 10 different random initial configurations for 150 ns. The random initial configurations were taken from an initial 100 ns production run using the settings described in section 2.2 of the main manuscript at 3 M TMAO concentration. Errors were calculated using block averaging over 10 preferential binding coefficients obtained from each run. Preferential binding coefficients of the single helix have been doubled to obtain the preferential binding coefficient of the dissociated state. The preferential binding coefficients of TMAO for the helices interacting through WCA, vdW and, vdW and electrostatic (Full) interactions are shown in Fig. S3. TMAO preferentially binds ($\Gamma_{23} > 0$) to the repulsive helix cavity, which would lead to a decrease of $\Delta\Delta G_{\mathrm{vdW,R}}$ (see eqn S6). The preferential TMAO binding increases with the introduction of attractive van der Waals interactions. On the other hand, TMAO is depleted from the fully interacting helix (van der Waals (vdW) and electrostatics, $\Gamma_{23} < 0$), which would lead to an increase of $\Delta\Delta G$ at high TMAO concentrations. These qualitative predictions, which are based on the results in Fig. S3 and eqn S6, are in agreement with the solvation free energy calculations (Fig. 2, 3, S4, S6).

S7 Contribution to the solvation free energy from cohesive van der Waals interactions $\Delta\Delta G_{\mathrm{vdW,A}}$

Figure S4(a) shows the dependence of $\Delta\Delta G_{\mathrm{vdW,A}}$ on the TMAO concentration for the associated and dissociated states. $\Delta\Delta G_{\mathrm{vdW,A}}$ decreases at a faster rate for the dissociated state than for the associated state, which in turn shifts the $D \rightleftharpoons A$ equilibrium towards the dissociated state i.e. $\Delta\Delta G^{\mathrm{D}\to\mathrm{A}}_{\mathrm{vdW,A}}$ increases with increase in TMAO concentration (Figure S4(b)). This occurs due to the larger SASA of the dissociated state, as compared to the associated state, which leads to a larger number of favorable polyalanine-TMAO contacts.

S8 Free energies of introducing van der Waals and electrostatic interactions

From Figs. 2(a), 4 in the main text and Fig. S4, it can be seen that, with increase in TMAO concentration, the solvation free energies decrease when only solute-solvent van der Waals interactions are considered. The solute-solvent electrostatic interactions however counteract this favorable decrease in the solvation free energies as can be seen in Fig. S5.

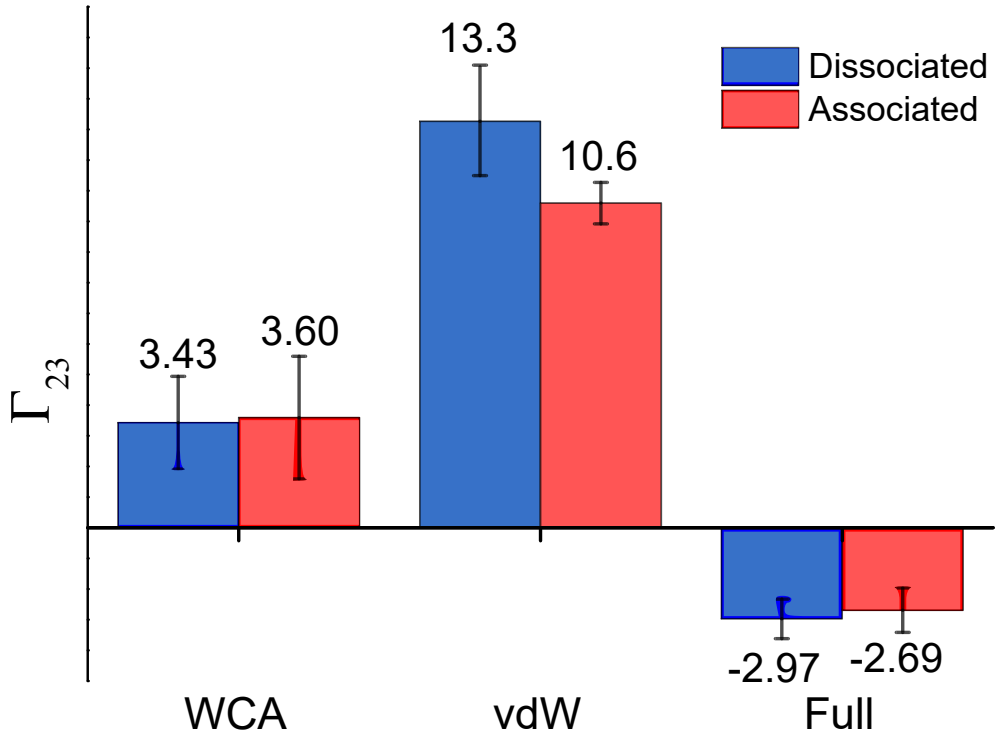

Fig. S3 Preferential binding coefficient Γ_{23} of TMAO at 3 M TMAO concentration for the associated and dissociated polyalanine helices. The preferential binding coefficient of TMAO for the helices interacting via WCA interactions is positive, showing preferential TMAO binding, as also indicated by the negative slope of $\Delta\Delta G_{\mathrm{vdW,R}}$. The introduction of attractive van der Waal interactions lead to an increase in the preferential binding coefficient (vdW). The preferential binding coefficient of TMAO for the helices interacting via van der Waals and electrostatic (full interactions) interactions is negative, showing TMAO depletion, as indicated by the positive slope of $\Delta\Delta G$ at high TMAO concentrations.

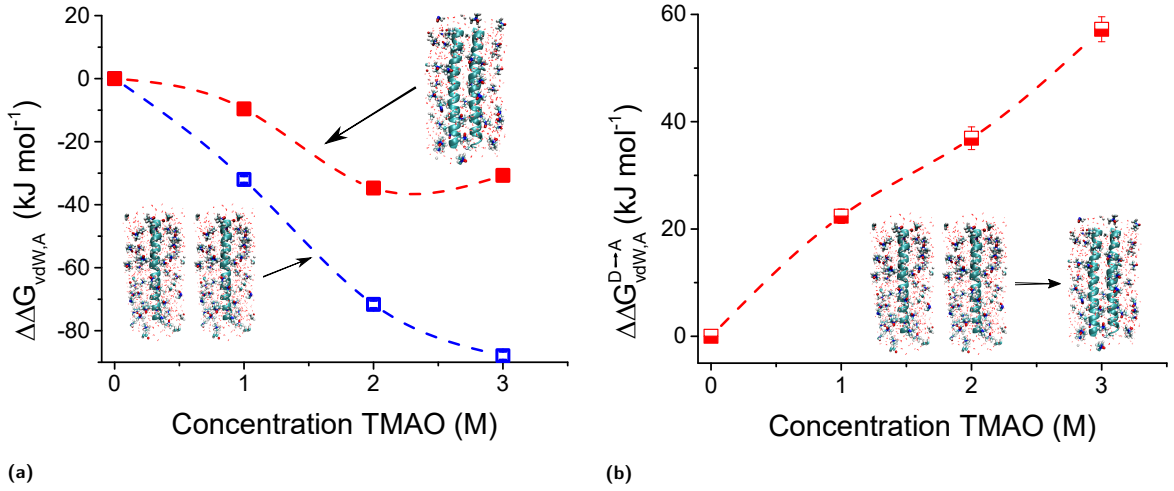

Fig. S4 a) Relative solvation free energy $\Delta\Delta G_{\mathrm{vdW,A}}$ as a function of TMAO concentration for the dissociated state ($\Delta\Delta G^{\mathrm{D}}_{\mathrm{vdW,A}}$, blue symbols) and the associated state ($\Delta\Delta G^{\mathrm{A}}_{\mathrm{vdW,A}}$, red symbols). The addition of TMAO has a bigger influence on $\Delta\Delta G^{\mathrm{D}}_{\mathrm{vdW,A}}$ due to its larger SASA. b) Dependence of the relative solvation free energy $\Delta\Delta G^{\mathrm{D}\to\mathrm{A}}_{\mathrm{vdW,A}}$, the attractive van der Waals interactions, on the TMAO concentration.

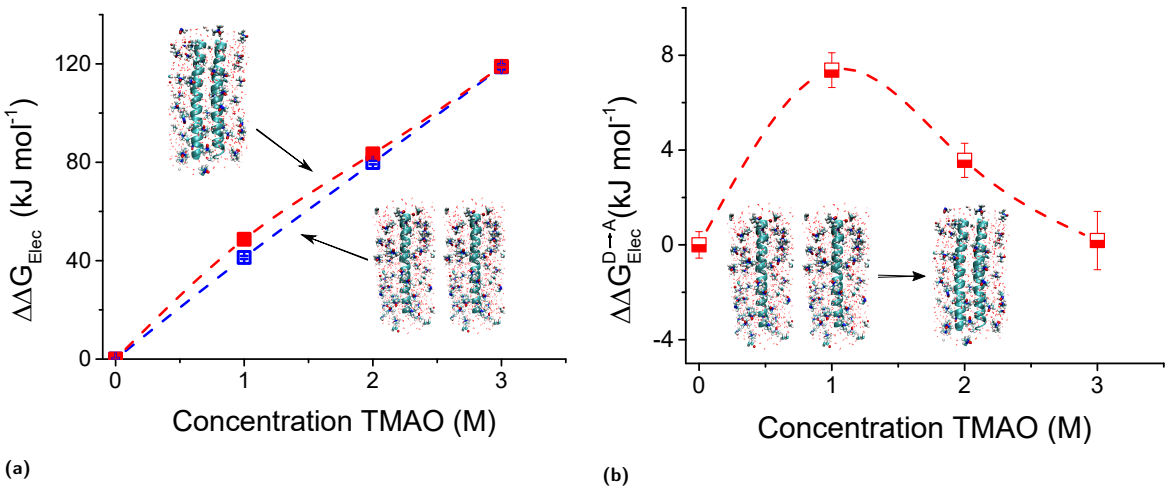

Fig. S5 a) Dependence of the relative solvation electrostatic free energy $\Delta\Delta G_{\text{Elec}}$ on TMAO concentration for the associated ($\Delta\Delta G^{\text{A}}_{\text{Elec}}$, red symbols) and dissociated ($\Delta\Delta G^{\text{D}}_{\text{Elec}}$, blue symbols) state. b) The relative solvation free energy of association $\Delta\Delta G^{\text{D}\to\text{A}}_{\text{Elec}} = \Delta\Delta G^{\text{A}}_{\text{Elec}} - \Delta\Delta G^{\text{D}}_{\text{Elec}}$ as a function of TMAO concentration. The positive slope in (a) indicates that TMAO accumulation is reduced by electrostatic interactions. The free energy of association in (b) reversely mirrors the trend in the free energy of solvation of van der Waals solutes (see Fig. 3(b)), leading to compensations between these two quantities.

This observation applies for, both, the associated and dissociated states. Therefore, the dependence of the relative solvation free energy of the fully interacting solute (van der Waals and electrostatic interactions), $\Delta\Delta G$, on the TMAO concentration is governed by the interplay of these two contributions that show compensating behaviors.

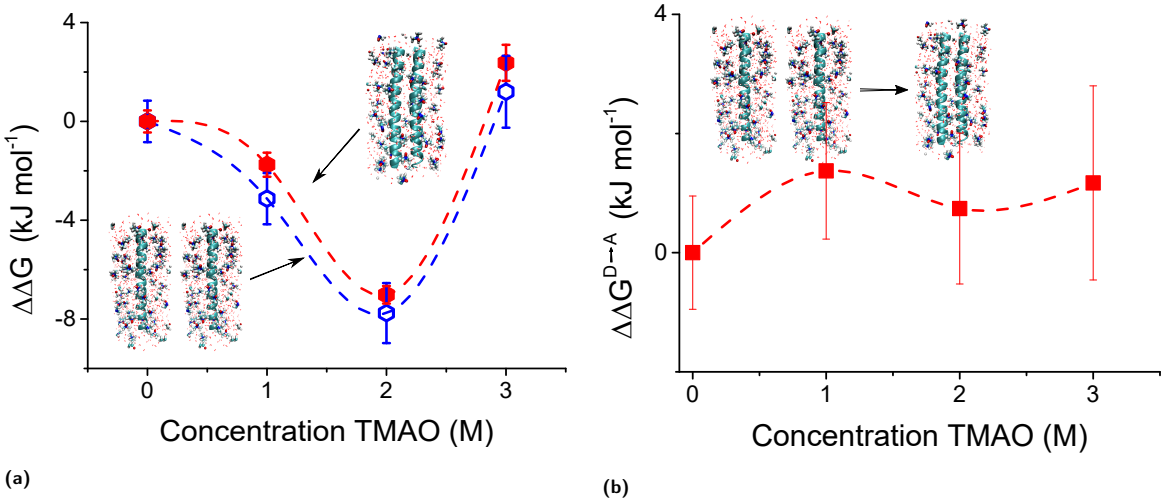

Fig. S6 a) Dependence of the relative solvation free energy $\Delta\Delta G$ on TMAO concentration for the associated ($\Delta\Delta G^{\text{A}}$, red symbols) and dissociated ($\Delta\Delta G^{\text{D}}$, blue symbols) polyalanine helices interacting through van der Waals and electrostatic interactions. b) The relative solvation free energy of association $\Delta\Delta G^{\text{D}\to\text{A}} = \Delta\Delta G^{\text{A}} - \Delta\Delta G^{\text{D}}$ as a function of TMAO concentration. The slope in a) is concentration dependent. The negative slope at low concentrations indicates preferential TMAO binding, while the positive slope indicates that at higher TMAO concentration, TMAO is depleted. The relative free energy of association for polyalanine does not display a clear trend but rather seems to remain constant.

The effect of this interplay can be seen in Fig. S6(a) where $\Delta\Delta G$, for both the associated and dissociated states, exhibits a non-monontonic dependence on the TMAO concentration. At low TMAO concentrations, $\Delta\Delta G$ decreases with increase in TMAO concentration indicating that the contribution from the solute-solvent van der Waals interactions is dominant (TMAO is preferentially adsorbed). On the other hand, at high TMAO concentrations, $\Delta\Delta G$ increases with increase in TMAO concentration which indicates that the contribution from the solute-solvent electrostatic interactions overcompensates the contribution from the solute-solvent van der Waals interactions (TMAO is depleted). From the dependence of $\Delta\Delta G^{\text{D}\to\text{A}}$ on the TMAO concentration in Fig. S6(b), it can be seen that the introduction of solute-solvent electrostatic interactions leads to the disappearance of the non-monotonic trends in $\Delta\Delta G^{\text{D}\to\text{A}}_{\text{vdW}}$ (see Fig. 3(b) of the main text).

Notes and references

1 J. D. Weeks, D. Chandler and H. C. Andersen, *J. Chem. Phys.*, 1971, **54**, 5237–5247.
2 P. V. Klimovich, M. R. Shirts and D. L. Mobley, *J. Comput. Aided Mol. Des.*, 2015, **29**, 397–411.
3 C. H. Bennett, *J. Comput. Phys.*, 1976, **22**, 245–268.
4 T. P. Straatsma and J. A. McCammon, *J. Chem. Phys.*, 1991, **95**, 1175–1188.
5 M. R. Shirts and J. D. Chodera, *J. Chem. Phys.*, 2008, **129**, 124105.
6 F. Eisenhaber, P. Lijnzaad, P. Argos, C. Sander and M. Scharf, *J. Comput. Chem.*, 1995, **16**, 273–284.
7 V. Pierce, M. Kang, M. Aburi, S. Weerasinghe and P. E. Smith, *Cell Biochem. Biophys.*, 2008, **50**, 1–22.
8 J. Wyman, *Adv. Prot. Chem.*, 1964, **19**, 223 – 286.
9 C. Tanford, *J. Mol. Biol.*, 1969, **39**, 539–544.
10 A. Ben-Naim, *Molecular theory of solutions*, Oxford University Press, Oxford, 2006.